nature climate change

LETTERS

https://doi.org/10.1038/s41558-017-0064-y

Corrected: Author correction

Biomass-based negative emissions difficult to reconcile with planetary boundaries

Vera Heck[1,2*], Dieter Gerten[1,2*], Wolfgang Lucht[1,2,3] and Alexander Popp[1]

Under the Paris Agreement, 195 nations have committed to holding the increase in the global average temperature to well below 2 °C above pre-industrial levels and to strive to limit the increase to 1.5 °C (ref. [1]). It is noted that this requires "a balance between anthropogenic emissions by sources and removals by sinks of greenhouse gases in the second half of the century"[1]. This either calls for zero greenhouse gas (GHG) emissions or a balance between positive and negative emissions (NE)[2,3]. Roadmaps and socio-economic scenarios compatible with a 2 °C or 1.5 °C goal depend upon NE via bioenergy with carbon capture and storage (BECCS) to balance remaining GHG emissions[4–7]. However, large-scale deployment of BECCS would imply significant impacts on many Earth system components besides atmospheric CO_2 concentrations[8,9]. Here we explore the feasibility of NE via BECCS from dedicated plantations and potential trade-offs with planetary boundaries (PBs)[10,11] for multiple socio-economic pathways. We show that while large-scale BECCS is intended to lower the pressure on the PB for climate change, it would most likely steer the Earth system closer to the PB for freshwater use and lead to further transgression of the PBs for land-system change, biosphere integrity and biogeochemical flows.

Negative emissions can fulfil several purposes. In a prospective, 2 °C or 1.5 °C warmer world with balanced sinks and sources of GHG emissions, they can allow for limited remaining fossil fuel use and/or compensate remaining agricultural or natural emissions (for example forest fires) or carbon leakages. If a complete decarbonization of the fossil fuel and agricultural sectors is achieved, NEs could reduce atmospheric CO_2 concentrations. BECCS is currently discussed as a promising NE technology[12]. It is therefore of considerable interest to examine the implications of NEs via BECCS in a holistic Earth system framework, such as the framework of a 'safe operating space'[10,11], delineated by nine PBs for human perturbations of the Earth system.

Here, we quantitatively assess trade-offs between BECCS and the status of five out of nine PBs for climate scenarios reaching 1.5 °C and 2 °C above pre-industrial. We consider the two PBs identified as core PBs, climate change and biosphere integrity[11], as well as the PBs for land-system change, biogeochemical flows and freshwater use, which are already transgressed except for freshwater use[11]. The latter four PBs have sub-global operating scales which are recognized in the definition of regional boundaries underpinning the global-level boundaries[11]. According to the precautionary principle, each PB is placed at the lower end of a scientific uncertainty range of its position. Upon transgression into the uncertainty zone, nonlinear shifts can no longer be excluded, while transgressing its upper end implies moving into a danger zone of high risk of irreversible shifts. To capture the importance of regional environmental change for the functioning of the Earth system we adopt the concept of a safe zone and a zone of increasing risk (uncertainty zone) also for the regional boundaries. These regional boundaries are: amount of remaining forest cover, biodiversity intactness index (BII), environmental flow requirements and imposed nitrogen fertilization limits, all calculated at the grid-cell level and subsequently aggregated to the analysis scale of regional boundaries (refer to Supplementary Table S2). We further compare our results to the originally defined global PBs.

Within this framework we distribute second-generation herbaceous or woody biomass plantations (irrigated or rainfed) using a spatially explicit multi-objective optimization approach in which biomass plantations can be allocated only on areas not required for food and feed production (see Methods). For this assessment, baseline agricultural land-use patterns are derived using the global land-use model MAgPIE[13,14] applied for the shared socio-economic pathways SSP1 (sustainability), SSP2 (middle of the road) and SSP5 (fossil-fueled development)[15] with and without climate policy to achieve RCP2.6 climate forcing levels (see Methods for details). Two alternative optimization objectives are examined: first, maximizing biomass production for NEs under the strict constraints of regional boundaries (safe) or the upper-end of their uncertainty zones (increasing risk); second, achieving certain biomass production for NE while minimizing the pressure on global PBs. We measure the state of the Earth system with respect to each PB via the global and regional control variables (Supplementary Table S2). The optimized biomass plantation patterns are combined with the agricultural baselines and assessed for PB impacts with the well-established biogeochemical model LPJmL, driven by an ensemble of climate scenarios scaled to reach a global warming of 1.5 °C and 2 °C in the second half of the century[16] and capturing differences in the spatial patterns produced by 19 climate models (see Methods). Results are averaged over 2051–2082 (covering four harvest cycles). To obtain NE and bioenergy potentials we consider two alternative conversion pathways: biomass conversion to hydrogen (B2H2) with high capture rates (90%) and conversion efficiencies (55%), and conversion to liquid fuels (B2L) with lower capture rates (48%) and efficiencies (41%) [ref. [17] and see Methods]. Input of fossil fuels for biomass production and transportation is assumed to be 10% of the primary energy content[18,19].

In all agricultural baseline scenarios (SSP patterns excluding biomass plantations for 2050) the global PBs for climate change, biosphere integrity, land-system change and nitrogen flows are transgressed even further than at present. Thus, in a strict sense, NEs via BECCS are not compatible with navigation of human development within the safe operating space for the agricultural land-use scenarios assessed, as BECCS would put additional pressure on the PBs.

[1]Potsdam Institute for Climate Impact Research, Potsdam, Germany. [2]Department of Geography, Humboldt-Universität zu Berlin, Berlin, Germany. [3]Integrative Research Institute on Transformations of Human–Environment Systems, Berlin, Germany. *e-mail: heck@pik-potsdam.de, gerten@pik-potsdam.de

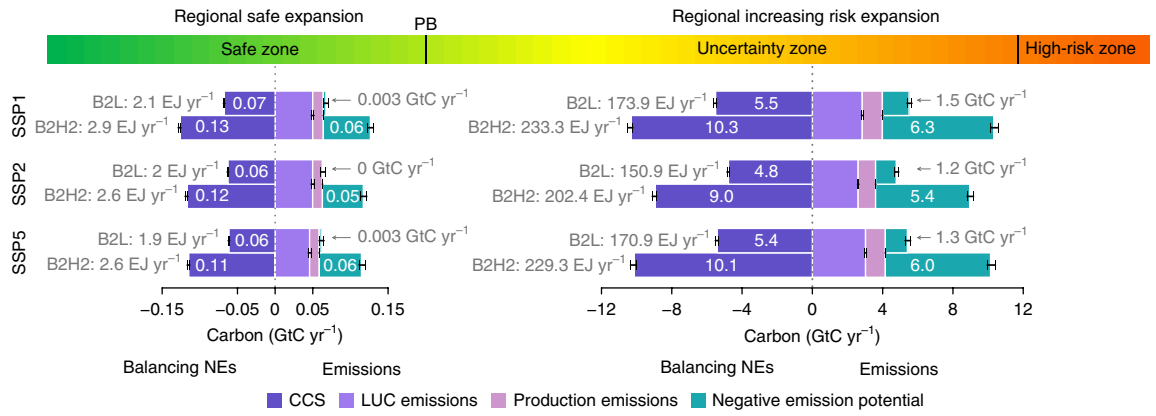

Fig. 1 | Emission balance of optimal biomass production within regional safe and increasing risk zones for two biomass conversion pathways. Biomass production is maximized around the agricultural baselines of SSP1, SSP2 and SSP5 (including climate policy of achieving RCP2.6 climate forcing levels) for 2050. NE potentials from biomass conversion to hydrogen (B2H) or liquid (B2L) are derived from CCS potentials, subtracting emissions associated with LUC, production and transportation of biomass. Bioenergy potentials (in exajoules) are calculated from biomass harvest and conversion efficiencies (Methods). Error bars reflect the range stemming from 19 climate scenarios with a global warming of 1.5 °C for 2050–2082 (see details in Methods).

However, the PB for climate change was identified as a core boundary, the transgression of which can have substantial consequences for the status of other boundaries and drive the Earth system out of the Holocene state[11]. Therefore, it might be feasible to counteract climate change while accepting some collateral transgression. As a minimal requirement, however, we assume that regional boundaries should not be altered to a state outside of their uncertainty ranges, to avoid feedbacks to large-scale processes[11].

We evaluate safe biomass-based NEs while ensuring adherence of biomass plantations to either the regional safe or uncertainty zones. The range of resulting potentials for NE via BECCS is large (Fig. 1). In the regional safe zone, small opportunities for biomass plantations, conditioned by the agricultural baseline scenarios, result in marginal CCS potentials of 0.11 GtC yr^{-1} to 0.13 GtC yr^{-1} with a highly efficient conversion to hydrogen (B2H2, Fig. 1). Taking into account the related land use change (LUC) emissions and input of fossil fuels for production, the resulting actual NE potential is <0.1 GtC yr^{-1} for all land-use baselines (Fig. 1), corresponding to ~0.5% of current carbon emissions. Thus, if regional safe zones are adhered to, BECCS can only marginally contribute to balancing remaining emissions or reducing atmospheric CO_2 concentrations.

Allowing the more risky exploitation of the full uncertainty zones of the regional boundaries considered increases the potential for NEs via BECCS significantly. With the highly efficient B2H2 pathway, the CCS potential in the assessed SSP scenarios ranges from 9.0 GtC yr^{-1} to 10.3 GtC yr^{-1} (Fig. 1) while producing 202 EJ yr^{-1}–233 EJ yr^{-1} in the form of hydrogen. Conversion to liquid fuels halves the CCS potentials and lowers bioenergy production by 25%. The actual NE potential, however, is smaller than the CCS potential because of substantial LUC emissions of 2.8 GtC yr^{-1} (averaged over a 32-year timespan) and emissions associated with biomass production and transportation (Fig. 1). Thus, in 2050, NEs of 1.2 GtC yr^{-1}(B2L, SSP2) up to 6.3 GtC yr^{-1} (B2H2, SSP1) could be achieved via BECCS in a riskier strategy that discards the precautionary principle and could trigger critical environmental feedbacks to the Earth system.

Despite fundamental differences in the SSP storylines, the potentials for BECCS are remarkably similar for the SSP1, SSP2 and SSP5 agricultural baselines, albeit the largest BECCS potentials can be achieved in the SSP1 sustainability scenario. In all scenarios, the climate policies implemented towards an RCP2.6 climate forcing result in smaller agricultural land demands, and thus larger NE potentials compared to the reference SSP scenarios without climate policy (Supplementary information). If these NEs were completely used for balancing fossil fuel emissions, primary energy of 48 EJ yr^{-1} to 258 EJ yr^{-1} from coal could be offset (based on an emission factor of 90 gCO_2-eq/MJ_{th} for coal[20]), depending on the biomass conversion pathway and socioeconomic land-use scenario. This wide range of NE potentials reflects major uncertainties related to the mix of BECCS technologies, and smaller uncertainties related to future land-use change for agriculture.

Due to the considerable reduction of CCS potentials by LUC emissions (Fig. 1) we further performed the optimization with a modified objective of maximizing the net flux of biomass production minus LUC emissions. Overall, this increases NE potentials slightly (+2% for B2H2 and +27% for B2L in SSP1) because of avoided LUC emissions (Supplementary Fig. 2). Optimized biomass potentials, however, are smaller than those of biomass harvest optimization neglecting LUC effects. This reduces CCS rates and bioenergy generation by 7%. These findings highlight a trade-off between NE and bioenergy production: although NE potentials are higher if LUC emissions are considered, bioenergy production potentials decrease.

Our optimization allows allocation of biomass plantations only in regions where the agricultural baselines' impacts are small enough to allow for additional biomass plantations within regional safe or uncertainty zones of biosphere integrity, biogeochemical flows, land-system change and freshwater use (Supplementary Fig. 1). Even though regional environmental limits are being considered, allocation of additional biomass plantations adds to the transgression of boundaries at the global scale. Figure 2 illustrates that in the process of decreasing the pressure on the PB for climate change with BECCS, additional pressure is exerted onto other PBs. With the regional safe constraint, almost no biomass plantations can be implemented. Thus, the values of the PB control variables are almost the same as in the agricultural baseline of SSP1 (dashed blue line). Under the constraint allowing for exploitation of regional uncertainty zones, many global PB control variables are severely impacted while the NE potential increases, especially under the highly efficient biomass conversion pathway to hydrogen (B2H2) (Fig. 2).

In the scenario allocating biomass plantations around the SSP1 and SSP2 agricultural baseline and allowing for a transgression of regionally safe environmental limits up to the upper end of the regional uncertainty zones, biomass plantations are allocated on

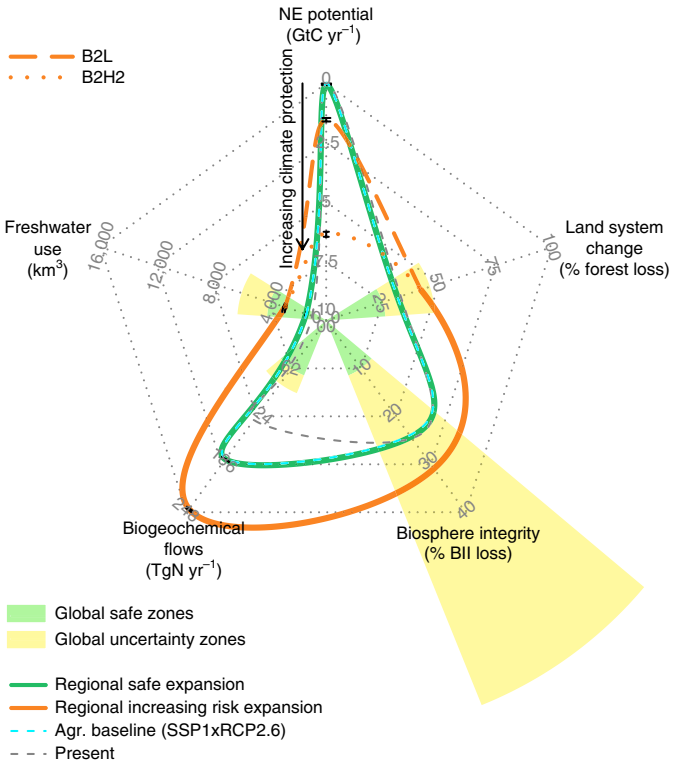

Fig. 2 | Status of global PBs considering agricultural land use in SSP1 and biomass production within regional safe and increasing risk zones. Optimally allocated biomass plantations for 2050 under the constraints of staying within regional safe (green line) and uncertainty zones (orange lines) are combined with the SSP1xRCP2.6 agricultural baseline for food and feed production (dashed blue). The present (2005) status of the PBs (dashed grey) is calculated based on the MAgPIE model initialization (see Methods). NE potentials are depicted for the biomass conversion to hydrogen (B2H2) and liquid (B2L). Error bars reflect the range under forcing from 19 climate scenarios reaching a global warming of 1.5 °C (see Methods). Green and yellow planes indicate the global safe and uncertainty zones[11].

870 Mha and 778 Mha, respectively. This increases land-use area by 19% (SSP1) and 17% (SSP2) compared to the agricultural baseline, with additional forest loss on 645 Mha, increasing the transgression of the land-system-change boundary (+10% forest loss, SSP1) and 586 Mha (+9% forest loss, SSP2). This adds significant pressure on biodiversity (+7% loss of biodiversity intactness, see Methods). The biomass potential largely stems from herbaceous biomass with relatively low nitrogen requirements[21]. Nonetheless, fertilizer requirements further alter global biogeochemical flows (+65 TgN yr^{-1} (SSP1) and + 56 TgN yr^{-1} (SSP2) fertilization). Most of the biomass plantations are set to be irrigated because regional water availability, even if accounting for environmental flow requirements, is generally high in productive regions without large agricultural water appropriation. Consequently, water consumption by biomass plantations more than doubles agricultural water consumption (+1167 km^3). Such massive irrigation benefits productivity of biomass plantations (on average 22 tDM ha^{-1}), reducing land requirements and impacts on biodiversity. However, a large share of irrigated areas is allocated to development countries where installation of large-scale modern irrigation technologies may be economically challenging.

We assess the interactions between freshwater use, biodiversity conservation and land-system change in more detail (Fig. 3 for the SSP1 baseline, see Supplementary Information for other agricultural baselines). For this, we adopt the alternative optimization objective prescribing a certain biomass harvest while minimizing the pressure on different global PBs disregarding regional constraints.

The pressure added to the boundaries of freshwater use, biosphere integrity and land-system change is sensitive to the prioritization of different conservation objectives, indicating trade-offs between the individual priorities. When prioritizing global biodiversity conservation (Fig. 3a), biomass plantations are mostly allocated on grasslands or savannahs with relatively low species richness. High biomass targets (up to 20 GtC yr^{-1} can thus be met without much further deterioration of biosphere integrity and land-system change but would require massive irrigation of biomass plantations (accounting for regional water availability but disregarding environmental flow requirements). Global water consumption transgresses the PB for freshwater use for targeted biomass production >5 GtC yr^{-1} and exits the global uncertainty zone for biomass production >10 GtC yr^{-1} (Fig. 3a).

Prioritizing freshwater conservation (Fig. 3b) leads to significant water-saving potentials for the same biomass production (2150–6000 km^3 yr^{-1}), because biomass plantations are allocated to productive regions with smaller water deficits. This implies, however, high forest loss, especially in the tropics, increasing biosphere integrity loss (by an additional 2–10%) and land-system change (3–21% additional forest loss, Fig. 3b). Furthermore, land-use-change emissions from deforestation result in overall smaller NE potentials.

All simulated NE potentials are to be considered rather optimistic because they imply implementation of large-scale modern irrigation and fertilization management of second-generation biomass plantations. Logistic and economic challenges related to management, possible carbon storage rates or the availability of geological storage sites near biomass plantations are not accounted for. Furthermore, BECCS potentials are subject to large uncertainties regarding the potential scale, conversion efficiencies, economic feasibility, as well as public and legal acceptance[22,23]. Currently only a few BECCS sites exist, and even obtaining the relatively small biomass to liquid efficiencies (B2L) would require substantial upscaling and development of CCS technologies[22].

Integrated assessment studies project total NE requirements of 0.6 to 4.1 GtC yr^{-1} (0.5 to 2.7 GtC yr^{-1}) in 2050 for limiting global warming to 1.5 °C (2 °C)[5,24], with a substantial increase throughout the century. Our internally consistent biogeochemical simulation results shed light on the feasibility and trade-offs of a BECCS contribution from dedicated bioenergy crops to NE requirements for three alternative storylines of future land-use development. We have shown substantial trade-offs between BECCS and PBs at regional and global scales, complementing previous assessments of biophysical limitations[25] and trade-offs with food production[26], biodiversity[27] and water use[28].

In conclusion, if regional boundaries were adopted as precautionary environmental guardrails, the potential for NEs from dedicated bioenergy plantation is marginal (<0.1 GtC yr^{-1}). The NE requirements projected could be met only if the precautionary principle of the planetary boundaries framework was discarded, and if highly efficient biomass conversion to hydrogen and carbon storage pathways were available. This shows that socio-economic pathways requiring substantial BECCS bear the risk of triggering potentially irreversible changes in the Earth system through extensive land-use change, water use, alteration of biogeochemical flows and compromising biosphere integrity. Pending ongoing improvements in the definition and quantification of PBs[11], relying on BECCS as a key decarbonization strategy should be considered highly risky. Thus, early and ambitious GHG reductions, rapid development of less invasive NE technologies[29] and use of other feedstocks for BECCS (for example, residues) are required to maintain a chance of keeping global warming well below 2 °C.

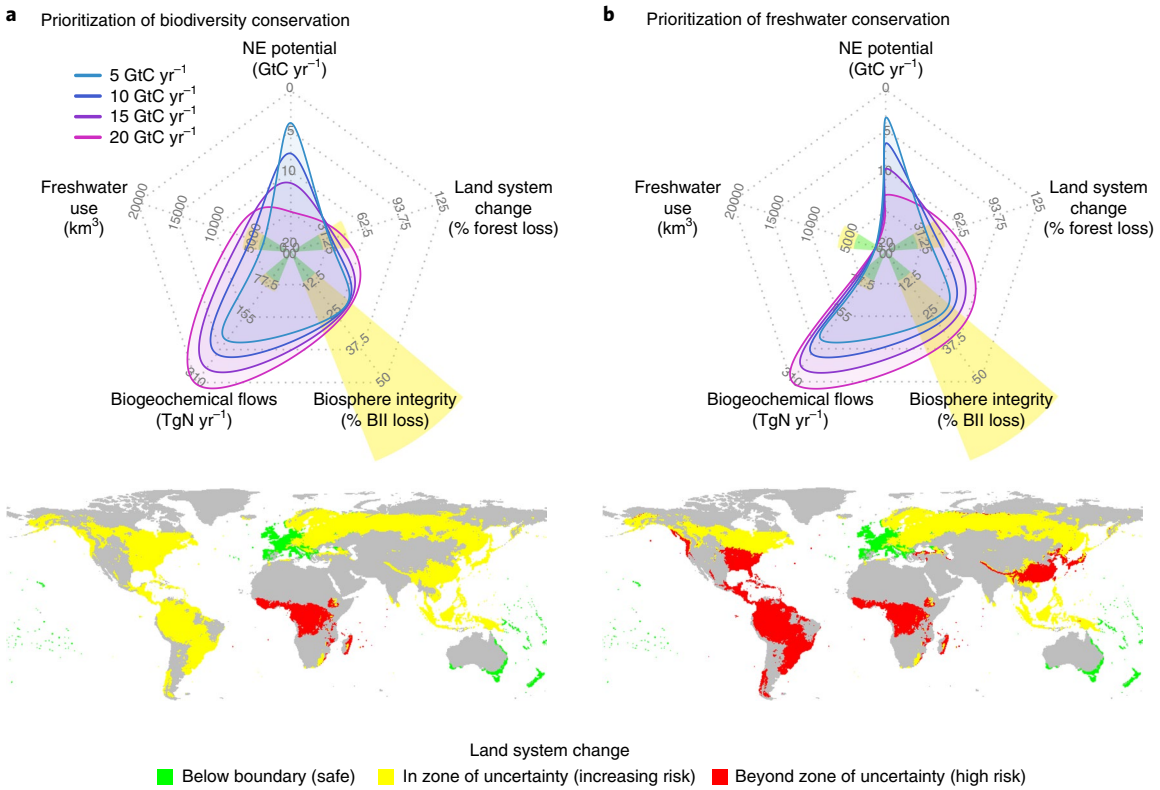

Fig. 3 | Effect of biodiversity and freshwater conservation objectives for fixed biomass production targets. Fixed biomass production targets reached under prioritization of biodiversity conservation (**a**) and prioritization of freshwater conservation (**b**). Biomass plantations are distributed around the SSP1xRCP2.6 agricultural baseline with a global warming of 1.5 °C. NE potentials are depicted for the highly efficient biomass conversion pathway to hydrogen (B2H2). Maps show exemplarily the regional status of the control variable for land-system change optimized for a global biomass production of 15 GtC yr^{-1} under the respective conservation objective.

Methods

Methods, including statements of data availability and any associated accession codes and references, are available at https://doi.org/10.1038/s41558-017-0064-y.

Received: 23 September 2016; Accepted: 18 December 2017;
Published online: 22 January 2018

References

1. *Adoption of the Paris Agreement* FCCC/CP/2015/L.9/Rev1 (UNFCCC, 2015).
2. Rogelj, J. et al. Zero emission targets as long-term global goals for climate protection. *Environ. Res. Lett.* **10**, 105007 (2015).
3. Sanderson, B. M., O'Neill, B. C. & Tebaldi, C. What would it take to achieve the Paris temperature targets? *Geophys. Res. Lett.* **43**, 7133–7142 (2016).
4. Rockström, J. et al. A roadmap for rapid decarbonization. *Science* **355**, 1269–1271 (2017).
5. Fuss, S. et al. Betting on negative emissions. *Nat. Clim. Chang.* **4**, 850–853 (2014).
6. Gasser, T., Guivarch, C., Tachiiri, K., Jones, C. D. & Ciais, P. Negative emissions physically needed to keep global warming below 2 °C. *Nat. Commun.* **6**, 7958 (2015).
7. Popp, A. et al. Land-use futures in the shared socio-economic pathways. *Glob. Environ. Chang.* **42**, 331–345 (2017).
8. Vaughan, N. E. & Lenton, T. M. A review of climate geoengineering proposals. *Climatic Change* **109**, 745–790 (2011).
9. Heck, V., Gerten, D., Lucht, W. & Boysen, L. R. Is extensive terrestrial carbon dioxide removal a 'green' form of geoengineering? A global modelling study. *Glob. Planet. Chang.* **137**, 123–130 (2016).
10. Rockström, J. et al. A safe operating space for humanity. *Nature* **461**, 472–475 (2009).
11. Steffen, W. et al. Planetary boundaries: guiding human development on a changing planet. *Science* **347**, 1259855 (2015).
12. Schleussner, C. F. et al. Science and policy characteristics of the Paris Agreement temperature goal. *Nat. Clim. Chang.* **6**, 827–835 (2016).
13. Kriegler, E. et al. Fossil-fueled development (SSP5): an energy and resource intensive scenario for the 21st century. *Glob. Environ. Chang.* **42**, 297–315 (2017).
14. Popp, A. et al. Land-use protection for climate change mitigation. *Nat. Clim. Chang.* **4**, 1095–1098 (2014).
15. Riahi, K. et al. *Glob. Environ. Chang.* **42**, 153–168 (2017).
16. Heinke, J. et al. A new climate dataset for systematic assessments of climate change impacts as a function of global warming. *Geosci. Model. Dev.* **6**, 1689–1703 (2013).
17. Klein, D. et al. The value of bioenergy in low stabilization scenarios: an assessment using REMIND-MAgPIE. *Climatic Change* **123**, 705–718 (2014).
18. Edenhofer, O. et al. (eds.) *Renewable Energy Sources and Climate Change Mitigation* (Cambridge University Press, Cambridge, 2011).
19. Qin, X., Mohan, T., El-Halwagi, M., Cornforth, G. & McCarl, B. A. Switchgrass as an alternate feedstock for power generation: an integrated environmental, energy and economic life-cycle assessment. *Clean. Technol. Environ. Policy* **8**, 233–249 (2006).
20. National Greenhouse Gas Inventories Programme *IPCC Guidelines for National Greenhouse Gas Inventories* (IPCC, 2006).
21. Roncucci, N., Nassi O Di Nasso, N., Tozzini, C., Bonari, E. & Ragaglini, G. *Miscanthus giganteus* nutrient concentrations and uptakes in autumn and winter harvests as influenced by soil texture, irrigation and nitrogen fertilization in the Mediterranean. *Glob. Chang. Biol. Bioenergy* **7**, 1009–1018 (2015).
22. Herzog, H. J. Scaling up carbon dioxide capture and storage: from megatons to gigatons. *Energy Econ.* **33**, 597–604 (2011).
23. Watson, J., Kern, F. & Markusson, N. Resolving or managing uncertainties for carbon capture and storage: Lessons from historical analogues. *Technol. Forecast. Soc.* **81**, 192–204 (2014).
24. Rogelj, J. et al. Energy system transformations for limiting end-of-century warming to below 1.5 °C. *Nat. Clim. Chang.* **5**, 519–527 (2015).
25. Smith, P. et al. Biophysical and economic limits to negative CO_2 emissions. *Nat. Clim. Chang.* **6**, 42–50 (2016).
26. Smith, P. et al. How much land-based greenhouse gas mitigation can be achieved without compromising food security and environmental goals? *Glob. Chang. Biol.* **19**, 2285–2302 (2013).

27. Beringer, T., Lucht, W. & Schaphoff, S. Bioenergy production potential of global biomass plantations under environmental and agricultural constraints. *Glob. Chang. Biol. Bioenergy* **3**, 299–312 (2011).
28. Bonsch, M. et al. Trade-offs between land and water requirements for large-scale bioenergy production. *Glob. Chang. Biol. Bioenergy* **8**, 11–24 (2014).
29. Woolf, D. et al. Sustainable biochar to mitigate global climate change. *Nat. Commun.* **1**, 56 (2010).

Acknowledgements

We thank H. Kreft and C. Meyer for providing the endemism richness data sets and B. Bodirsky for discussions on the planetary boundary for biogeochemical flows. This research was funded by the DFG in the context of the CE-Land and CEMICS2 projects of the Priority Program 'Climate Engineering: Risks, Challenges, Opportunities?' (SPP 1689). We acknowledge the European Regional Development Fund (ERDF), the German Federal Ministry of Education and Research and the Land Brandenburg for supporting this project by providing resources on the high-performance computer system at the Potsdam Institute for Climate Impact Research.

Author contributions

V.H. designed the study with input from D.G., W.L. and A.P. V.H. developed the methodology, performed all simulations, analysed the results and created the figures. Land-use data from MAgPIE were provided by A.P. V.H. led the writing process with contributions from D.G., W.L. and A.P.

Competing interests

The authors declare no competing financial interests.

Additional information

Supplementary information is available for this paper at https://doi.org/10.1038/s41558-017-0064-y.

Reprints and permissions information is available at www.nature.com/reprints.

Correspondence and requests for materials should be addressed to V.H.

Publisher's note: Springer Nature remains neutral with regard to jurisdictional claims in published maps and institutional affiliations.

Methods

We developed a multi-objective optimization model for the spatial allocation of biomass plantations. The model is based on simulations with the state-of-the-art dynamic vegetation model LPJmL, scenarios of baseline agricultural land use patterns for food production, and data sets on indicators of biodiversity. The optimization is driven by constraints and objectives according to global and regional representations of the planetary boundaries for biosphere integrity, biogeochemical flows, land-system change and freshwater use. The optimization model and its foundations are described in more detail in the following sections.

The dynamic vegetation model LPJmL. LPJmL represents natural ecosystems and managed croplands including biomass plantations to simulate key ecosystem processes and coupled carbon and hydrological cycles[30,31]. It has been extensively validated for carbon cycles[32], agricultural crop and biomass production[9,33,34], water flows and irrigation requirements[30,31]. Biomass plantations are a representation of highly productive herbaceous and woody second-generation biomass plantations, validated in refs [9,27]. Their parameterizations are based on observations of the growth and harvest characteristics of Miscanthus/switchgrass cultivars for the herbaceous biomass plantations, and willows/poplars and Eucalyptus plantations for temperate and tropical woody biomass plantations, respectively. Herbaceous biomass plantations are simulated to be harvested on a multi-annual basis, and woody biomass plantations every eight years with a plantation rotation time of 40 years.

LPJmL was applied to determine the potential changes in carbon pools and fluxes under conversion to biomass plantations, potential irrigation water requirements of biomass plantations and water availability for irrigation, as well as biogeochemical and hydrological impacts of the agricultural baseline scenarios. All simulations were preceded by a 5000-year spin-up with natural vegetation, bringing soil carbon pools and vegetation distribution into equilibrium. A subsequent second spin-up period of 390 years introduces historical agriculture with annual cropland extent and crop type distribution per 0.5° grid cell and irrigated fraction per crop type after ref. [35] from 1700–2005, allowing for a historical adjustment of carbon pools. During the spin-ups, the climate (historical climate data from CRU TS3.10[36] of the years 1901–1930) was repeated. Further simulations from 2005–2050 serve as spin-ups for the actual simulations using the different baseline agricultural land-use patterns without biomass plantations and a temperature-stratified climate scenario with a global warming of 2 K during the 30-year-mean around 2100, reproducing the median response of 19 general circulation models[16]. LPJmL simulations and their purpose for the optimization are summarized in Supplementary Table S1.

Biomass plantations are cultivated in regions where climate conditions allow biomass harvests >5 tDM ha^{-1} yr^{-1} (ref. [37]). For the generation of optimization inputs one medium-range climate model (MPI-ESM) is used to simulate changes in soil and vegetation carbon pools related to biomass plantations and deforestation, potential irrigated and rainfed biomass yields, potential water consumption of irrigated biomass plantations and regional water availability.

To allow for consistent biogeochemical and hydrological modelling, all optimized land-use patterns were simulated by LPJmL from 2051 to 2082 (that is, four harvest cycles of woody biomass plantations) on a spatial resolution of 0.5°, driven by an ensemble of 19 temperature-stratified climate scenarios with a global warming of 1.5 K and 2 K during the 30-year-mean around 2100[16]. In case of deforestation for biomass plantations, the natural vegetation replaced is treated as a one-time biomass harvest which is used as feedstock for BECCS.

Calculation of negative emission potentials. In BECCS systems, the harvested biomass can be converted to different types of secondary energy carriers via multiple technology pathways that allow for carbon capture and subsequent carbon storage, for example, in underground reservoirs. We consider two biomass conversion technologies: biomass conversion to hydrogen (B2H2) and biomass conversion to liquid fuels (B2L), which form the upper (B2H2) and lower (B2L) end of bioenergy conversion and carbon capture efficiencies[17]. B2H2 has potentially very high capture rates (up to 90%) because hydrogen is a carbon-free secondary energy carrier. In contrast B2L has a low capture rate (up to 48%) since the resulting fuel contains a significant share of carbon. Fossil fuel input to biomass production and transportation is assumed to be constant at 10% of the primary energy content[18,19].

The annual NE potential (P_{NE}) is calculated via:

$$P_{NE} = C_r \frac{H_{cum} - E_{LUC} - E_P}{n_y} \quad (1)$$

with c_r: capture rate, H_{cum}: biomass harvest, E_{LUC}: land-use-change emissions and E_p: production and transportation emissions. The cumulative biomass harvest (H) includes one-time-harvested timber from deforestation and cumulative harvest from biomass plantations. Land-use-change emissions are carbon emissions (soil and vegetation) due to land-use change from natural vegetation to biomass plantations, computed by LPJmL.

Agricultural baseline scenarios. The agricultural baseline consists of land-use patterns for food and feed production for SSP1, SSP2 and SSP5 under no-mitigation (reference) and ambitious mitigation (RCP 2.6), derived by the Model of Agricultural Production and its Impacts on the Environment (MAgPIE) for 2050[14,38]. These SSPs depict three different global futures with substantially different socio-economic conditions that aim to reflect different socio-economic challenges to mitigation and are of greatest interest to assess BECCS potentials. SSP1 describes a sustainable future in which environmental boundaries are respected, including climate change mitigation (RCP2.6 in the baseline) and hence bioenergy needs. SSP2 represents a world that follows a middle-of-the-road pathway with intermediate challenges for mitigation, whereas SSP5 describes a resource intensive world with high GHG emissions (RCP8.5 in the baseline), high challenges mitigation and hence bioenergy needs. Land-use patterns are designed to ensure demand-fulfilling food production, where demand is externally prescribed based on extrapolation of historical relationships between population and GDP on national levels[39]. Land-based mitigation for MAgPIE is driven by carbon prices and bioenergy demand from the REMIND model as implemented in the SSP exercise[13] and affects agricultural land for food and feed production. Besides land-use patterns, also spatially explicit information on N-fixation and inorganic fertilizer on agricultural land have been provided by MAgPIE, based on a detailed nitrogen-budget model in consistency with SSP1, SSP2 and SSP5[40]. Spatially explicit agricultural water consumption is simulated by LPJmL, and non-irrigation human water consumption under the SSP2 scenario (415 km^3 in 2050) was provided by the WaterGAP model[41] and used for all agricultural baselines.

Optimization model. We developed an optimization model (based on the R-package *lpSolveAPI* for linear optimization[42]) that distributes herbaceous or woody biomass plantations (irrigated or rainfed) on a 0.5° grid around the fixed baseline agricultural land-use patterns, considering two alternative optimization objectives:

1) maximization of global biomass harvest (H) given fixed regional boundary constraints (C^{reg}_{PB}) of biosphere integrity (B), land system change (L), nitrogen flows (N) and freshwater use (W):

$$\max_{f_j \in C^{reg}_{PB}} \left(\sum_{j=1}^{n} \sum_{p} f_j^p \; h_j^p \right) \quad (2)$$

with f_j^p: cell fractions and h_j^p: harvest of biomass plantations $p \in$ {herbaceous irrigated, herbaceous rainfed, woody irrigated, woody rainfed} in gridcells $j = 1 \ldots n$. Biomass fractions are subject to regional constraints $\{C^{reg}_B, C^{reg}_L, C^{reg}_N, C^{reg}_W\}$.

2) minimization of impacts I on B, L, N, W for varied weights (w_{PB}) given fixed biomass harvest constraints (C^H):

$$\min_{f_j \in C^H} \left(\sum_{j=1}^{n} w_B I_j^B + w_L I_j^L + w_N I_j^N + w_W I_j^W \right), \quad (3)$$

with $C^H = \sum_{j=1}^{n} \sum_p f_j^p \; h_j^p \in \{5, 10, 15, 20\}$ GtC yr^{-1}.

Planetary and regional boundaries and optimization constraints. Under the first optimization objective (equation (2)), land-use expansion for bioenergy is allowed where regional environmental limits according to the planetary boundary concept are not transgressed in the agricultural baseline and until they are reached. The impacts on global control variables of the planetary boundaries are minimized in the second optimization objective (equation (3)). The global and regional control variables of the assessed PBs are summarized in the Supplementary Information (Supplementary Table S2).

Biogeochemical flows. The status of the global biogeochemical flows PB is approached via the intended nitrogen fixation (chemical N fixation in fertilizers and anthropogenically induced biological N fixation by legumes)[43]. As regional constraints we derive grid-cell-specific thresholds for nitrogen fixation considering the control variables used to assess the global PB for nitrogen flows[43]: atmospheric NH_3 concentrations and N concentrations in surface runoff (see Supplementary Table S2 for the proposed critical limits[43]). As proposed by de Vries et al.[43] we calculate critical global losses of a given N compound to either air or water by

$$N_{losses;crit} = N_{losses;present} \; RI_{Ncompound} \quad (4)$$

with the risk indicator $RI = [N]_{crit}/[N]_{present}$ and $[N]_{present}$ being the present concentration of the respective control variable. In contrast to de Vries et al.[43] we do not limit RI to values smaller than or equal to 1, as this would strictly forbid additional or initial fertilization in areas that are not close to the regional thresholds, thus forbidding fertilization on all primary and unfertilized land. Based on the respective range of critical limits, we obtain a range of global RI of 1.79–5.36 for atmospheric NH_3 concentrations and 0.61–1.53 for N in surface runoff using global average values of $NH_{3-present} = 0.56\,\mu g\,m^{-3}$ and $N_{runoff-present} = 1.63\,mg\,Nl^{-1}$[43]. Assuming that the ratio between N fixation and polluting compounds does not change[43], we multiply the respective RI by the agricultural nitrogen fixation of 121.5 Tg N in the year 2000[44]. To derive grid-cell-specific thresholds for nitrogen

fixation limiting NH_3 concentrations we divide the global critical value by the global land area. The grid cell threshold for limiting N runoff to surface waters is calculated by dividing the global critical value by surface runoff in the agricultural baseline scenario. Under the regional optimization constraints C_N^{reg}, biomass plantations can be allocated until the combined nitrogen fixation and fertilization of the agriculture baseline scenario and biomass plantations reaches one of the regional thresholds. Therefore, we derive nitrogen fertilizer requirements for biomass plantations from biomass harvest under the assumption that extracted nitrogen (0.15% N in dry matter for herbaceous biomass[21] and 0.5% N in dry matter for woody biomass[45]) is replenished with an efficiency of 50%[46].

Biosphere integrity. Several interim control variables have been proposed for the PB for biosphere integrity[11]. Acknowledging large uncertainties associated with the status of this PB, we calculate a measure similar to one of the proposed control variables, the biodiversity intactness index (BII)[11,47]:

$$BII = \frac{\sum_s \sum_l ER_s A_l I_{s,l}}{\sum_s \sum_l ER_s A_l}, \quad (5)$$

for species groups $s \in$ {amphibians, birds, mammals, vascular plants} and land cover $l \in$ {natural, cultivated, plantation}, with ER_s = endemism richness of species s, A_l = land area of land cover l and $I_{s,l}$ = intactness of species s with land cover l.

Endemic richness instead of proposed species richness is used to incorporate individual regional contributions to genetic diversity, which is the motivation for the second interim control variable[11]. Endemic richness data of terrestrial vertebrates were available on a 1° resolution and vascular plants for 90 terrestrial biogeographic regions[48]. Due to the lack of global impact data, we adopted expert impact estimates of South Africa[47] for a rough first estimate of species intactness on cultivated land or plantations. This implies that the absolute BII-values on the global or regional scale are highly uncertain. However, regional differences are respected in the spatial allocation of biomass plantations because the intactness estimates serve only as a factor to heterogeneously distributed endemic richness. The BII is calculated for the whole globe (global PB) and for 71 continental biomes. For the regional optimization constraint (C_B^{reg}) biomass plantations can be allocated in the respective biome as long as the BII (under combined agricultural and biomass plantation land use) is higher than 90% (safe limit) or 30% (uncertainty limit).

Freshwater use. The PB for freshwater use has two different control variables for the global and regional scale (human water consumption and environmental flow requirements, respectively). The basin-scale environmental water flows boundary limits blue water withdrawal along rivers to percentages of the mean monthly flow. It is calculated with the Variable Monthly Flow (VMF) method[49] accounting for intra-annual variability in terms of high-, intermediate- and low-flow months (ref. to Supplementary Table S2).

In the optimization, water availability for irrigation of biomass plantations is always limited at the grid-cell level and at the level of water basins. To account for upstream-downstream effects, upstream withdrawals (minus return flows) are subtracted from downstream water availability. Water availability is additionally limited at the basin level with an additional constraint that water withdrawals in each basin may not exceed the basin discharge. Without the regional boundary constraints, irrigation of biomass plantations is allowed to the extent of mean available water over the irrigation period after subtracting agricultural withdrawals and withdrawals for households, industry and livestock from the monthly water availability. This assumes that water can be stored during the irrigation period, but neglects irrigation water from fossil groundwater.

Under the regional boundary constraint on freshwater use (C_W^{reg}), the available water for irrigation of biomass plantations in each river basin is calculated as the mean available water over the irrigation period after subtracting monthly environmental flow requirements, agricultural withdrawals and withdrawals for households, industry and livestock from the monthly water availability. The same calculation is applied at the grid-cell level to limit water withdrawals and sustain environmental water flows at the grid-cell level.

Land-system change. The status of land-system change is derived from the potential forest cover simulated by LPJmL for historic climate data (CRU TS version3.1[36]). Regional constraints are on the scale of major forest biomes (tropical, temperate and boreal forests) of each continent (Supplementary Table S2). Under the global and regional land-system-change constraint, deforestation for biomass plantations is allowed as long as the respective global or regional boundary limits are not transgressed.

Data availability. The data that support the findings of this study are available from the corresponding author upon request.

References

30. Gerten, D., Schaphoff, S., Haberlandt, U., Lucht, W. & Sitch, S. Terrestrial vegetation and water balance—hydrological evaluation of a dynamic global vegetation model. *J. Hydrol.* **286**, 249–270 (2004).
31. Rost, S. et al. Agricultural green and blue water consumption and its influence on the global water system. *Water Resour. Res.* **44**, W09405 (2008).
32. Sitch, S. et al. Evaluation of ecosystem dynamics, plant geography and terrestrial carbon cycling in the LPJ dynamic global vegetation model. *Glob. Chang. Biol.* **9**, 161–185 (2003).
33. Bondeau, A. et al. Modelling the role of agriculture for the 20th century global terrestrial carbon balance. *Glob. Chang. Biol.* **13**, 679–706 (2007).
34. Fader, M., Rost, S., Müller, C., Bondeau, A. & Gerten, D. Virtual water content of temperate cereals and maize: present and potential future patterns. *J. Hydrol.* **384**, 218–231 (2010).
35. Jägermeyr, J. et al. Water savings potentials of irrigation systems: global simulation of processes and linkages. *Hydrol. Earth Syst. Sci.* **19**, 3073–3091 (2015).
36. Harris, I., Jones, P., Osborn, T. & Lister, D. Updated high-resolution grids of monthly climatic observations — the CRU TS3.10 Dataset. *Int. J. Climatol.* **34**, 623–642 (2014).
37. Hastings, A. et al. Future energy potential of Miscanthus in Europe. *Glob. Chang. Biol. Bioenergy* **1**, 180–196 (2009).
38. Stevanovic, M. et al. The impact of high-end climate change on agricultural welfare. *Sci. Adv.* **2**, e1501452 (2016).
39. Bodirsky, B. et al. Food demand projections for the 21st century. *PLoS. One.* **10**, e0139201 (2015).
40. Bodirsky, B. et al. Reactive nitrogen requirements to feed the world in 2050 and potential to mitigate nitrogen pollution. *Nat. Commun.* **5**, 3858 (2014).
41. Flörke, M. et al. Domestic and industrial water uses of the past 60 years as a mirror of socio-economic development: A global simulation study. *Glob. Environ. Chang.* **23**, 144–156 (2013).
42. Konis, K. lpSolveAPI: R Interface to 'lp_solve' v.5.5.2.0 (2016); https://cran.r-project.org/web/packages/lpSolveAPI/index.html
43. de Vries, W., Kros, J., Kroeze, C. & Seitzinger, S. P. Assessing planetary and regional nitrogen boundaries related to food security and adverse environmental impacts. *Curr. Opin. Environ. Sustain.* **5**, 392–402 (2013).
44. Bouwman, L. et al. Exploring global changes in nitrogen and phosphorus cycles in agriculture induced by livestock production over the 1900–2050 period. *Proc. Natl Acad. Sci. USA* **110**, 20882–20887 (2011).
45. Kauter, D., Lewandowski, I. & Claupein, W. *Pflanzenbauwissenschaften* **5**, 64–74 (2001).
46. Lassaletta, L., Billen, G., Grizzetti, B., Anglade, J. & Garnier, J. 50 year trends in nitrogen use efficiency of world cropping systems: the relationship between yield and nitrogen input to cropland. *Environ. Res. Lett.* **9**, 105011 (2014).
47. Scholes, R. J. & Biggs, R. A biodiversity intactness index. *Nature* **434**, 45–49 (2005).
48. Kier, G. et al. A global assessment of endemism and species richness across island and mainland regions. *Proc. Natl. Acad. Sci. USA* **106**, 9322–9327 (2009).
49. Pastor, A. V., Ludwig, F., Biemans, H., Hoff, H. & Kabat, P. Accounting for environmental flow requirements in global water assessments. *Hydrol. Earth Syst. Sci.* **18**, 5041–5059 (2014).